Forging of Discontinuously Reinforced Aluminum Composites

A. Awadallah and J.J. Lewandowski, Case Western Reserve University

DISCONTINUOUSLY REINFORCED aluminum (DRA) alloy metal-matrix composites (MMCs) represent an advanced aluminum materials concept whereby ceramic particles, or whiskers, are added to aluminum-base alloys through the use of either ingot-melting or casting and/or powder-metallurgy (P/M) techniques. In these materials systems, the reinforcing material (for example, silicon carbide, boron carbide, or boron nitride) is not continuous, but consists of discrete particles within the aluminum alloy matrix. Unlike continuous metal-matrix composites, discontinuous metal-matrix composites can be deformation processed by all existing metalworking techniques, including forging. Addition of the reinforcement to the parent aluminum alloy matrix, typically in volume percentages from 10 to 40%, significantly modifies the properties of the alloy. Such additions significantly increase the elastic and dynamic moduli, increase strength, reduce ductility and fracture toughness, increase elevated-temperature properties, and do not significantly affect corrosion resistance. Recent summaries of the mechanical properties are provided elsewhere (Ref 1–3). Table 1 lists several of the developmental discontinuous metal-matrix composite materials systems that have been evaluated in forgings. Alloy and forging process development continues in order to facilitate commercial application of these materials.

Recent forging evaluation studies of these materials indicate that reinforcing additions to existing aluminum alloys modify the deformation behavior and increase flow stresses (Ref 5, 22, 23). The fabrication history of such materials may also affect their deformation behavior in forging in addition to altering the resulting mechanical properties. Although the recommended metal temperatures in forging these materials remain to be fully defined, current efforts suggest that temperatures higher than those listed in Table 2 for matrix alloys are typically necessary. Processing maps combining temperature and strain rate have been developed for some of the discontinuously reinforced aluminum- and magnesium-base systems (Ref 22). Forging evaluations have demonstrated that

discontinuous metal-matrix composites based on existing wrought aluminum alloys in the 2*xxx*, 6*xxx*, and 7*xxx* series can be successfully forged into all forging types, including high-definition and precision closed-die forgings. Some evidence suggests that these materials are more abusive of closed-die tooling and that die life in forging these materials may be shorter than is typical of the parent alloys (see the section "Forging Advanced Aluminum Materials" in the article "Forging of Aluminum Alloys" in this Volume).

There are a number of forged MMCs that are being explored for industrial use or are presently

Table 1   Aluminum-base discontinuous metal-matrix composite materials

Producer	Type	Matrix alloys	Reinforcements(a)	Reinforcement loading, vol%	Ref
Alcoa	P/M	2*xxx*	SiC_p	0–30	4
		7*xxx*	SiC_p	0–30	4
Dural	I/M	2014	SiC_p	0–40	4
		6061	SiC_p	0–40	4
		7075	SiC_p	0–40	4
DWA	P/M	2024	SiC_p	0–40	4
		6061	SiC_p	0–40	4
		7090	SiC_p	0–40	4
		7091	SiC_p	0–40	4
Silag	P/M	1100	SiC_w/SiC_p	0–30	4
		6061	SiC_w/SiC_p	0–30	4
		2124	SiC_w/SiC_p	0–30	4
		5083	SiC_w/SiC_p	0–30	4
		7075	SiC_w/SiC_p	0–30	4
		7090	SiC_w/SiC_p	0–30	4
		7091	SiC_w/SiC_p	0–30	4
Kobe	P/M-I/M	2024	SiC_w	0–30	4
		6061	SiC_w	0–30	4
		7075	SiC_w	0–30	4
Alcoa	P/M	7093	SiC	15	5, 19–21
		2080	SiC	15	5, 19–21
Dural Composites Corp	Cast + swaging	A356	SiC	20	6
Duralcan Inc	Direct chill cast and extruded	6061	Al_2O_3	20	7
Alcan	…	2618	SiC_p	14	8
Duralcan	Cast + extruded	2618	Al_2O_3	20	9
Chesapeake Composite Corp	Liquid-metal infiltration	DSC-A1	Al_2O_3	34, 37	10
Alcan	Cast	A359	SiC	20	11
Treibacher Schleifmittel, Germany	Gas pressure infiltration	A1	Al_2O_3	40–55	12
Not reported	Cast	A1	$Al_{62.5}Cu_{25}Fe_{12.5}$	5–20	13
Defense Metallurgical Research Laboratory	Degassed and compacted (CIP)	2124	SiC	20	14
Aerospace Metal Composite Limited	Hot isostatic pressing	2124	SiC	26	15
Not reported	Squeeze casting	6061	SiC	20	16
Duralcan Aluminum Composites Corp	Cast + extruded	2014	Al_2O_3	15	17
Not reported	Cast + forged	A1-5%Si -0.2%Mg	SiC_p	9–22	18

(a) SiC_w, whisker reinforcement; SiC_p, particulate reinforcement. Source: Ref 4–18

being used in industrial applications. Further information on general applications can be obtained in Ref 24 to 33. While many of the applications covered use MMCs that have been deformation processed, the applications utilizing forging are covered presently.

The Eurocopter rotor sleeve is an application that uses a forged SiC particulate reinforced 2*xxx* alloy having good stiffness and damage tolerance (Ref 34). It is a replacement for a titanium part with a reduction in weight and production cost. Another application utilizing the ability to match coefficient of thermal expansion with mating materials was the use of 6061/SiC/40p MMC in the covers for an aerospace inertial guidance unit. In this application, the MMC replaced beryllium that had to be machined from a solid block. The MMC material could be forged to near-net shape, with only final machining required (Ref 25).

Piston applications in automobile engines have included the use of SiC particulate reinforced aluminum forgings in racing applications. Due to the lower coefficient of thermal expansion of the MMC, reduced clearances between the piston and cylinder wall are possible. Based on trials of MMC pistons in drag racing bikes, improved performance compared to conventional hypereutectic aluminum-silicon alloys can result (Ref 25). Other drivetrain components, and particularly the connecting rod, have been a focus of development (Ref 25). By reducing the mass of the connecting rod/piston assembly, the objectionable secondary shaking forces that can develop particularly in smaller engines can be reduced. In addition, lower reciprocating loads should lead to lower loads on the crankshaft and lower friction losses, and increased fuel economy or performance can be realized (Ref 35). No commercial applications of connecting rods in high-volume vehicles have been achieved, largely because of the difficulty in obtaining a material with the necessary high-cycle fatigue performance and low-cost combination. While prototype connecting rods from

hot forged aluminum MMC have been prototyped and tested, further cost reduction is required (Ref 1–3).

This review begins with a summary of general observations on the forging of discontinuously reinforced composites, followed by a more detailed presentation of results obtained on specific alloy systems. A review of the efforts on the modeling of their behavior follows, with a comparison of experimental results to the modeling attempts. The resulting properties of forged materials are also presented when available.

General Information

Secondary processing such as forging and extrusion can improve the mechanical properties of MMC materials by breaking up particle agglomerates, reducing or eliminating porosity, and improving particle to particle bonding (Ref 6, 23). A potential problem with open-die forging is cracking that occurs on the outer surface, possibly due to secondary tensile stresses involved in forging that are imposed relatively quickly, resulting in matrix-reinforcement debonding, cavitation, reinforcement fracture, and macroscopic cracking (Ref 5, 19–21). Very high temperatures can also cause macro defects such as hot tearing or hot shortness (Ref 3, 23).

Predictions of the limiting strains during forging are provided in forging-limit diagrams popularized by Kuhn and Lee. in the 1970s (Ref 36). The diagrams are plots of tensile surface strain at the point of incipient surface cracking versus the applied compressive strain. An example of a forging-limit diagram of 6061 Al/20 vol% SiC and 6061 Al/20 vol% Al_2O_3 is shown in Fig. 1 (Ref 23). Additional processing maps have been developed and are summarized in Ref 22. These plots summarize the regimes of temperature and strain rate where various flow instabilities may occur. In this regard, such processing maps provide the safe combinations of temperature and strain rate to avoid various flow instabilities.

The enhancement of forgeability in particulate composites involves two main factors: matrix grain size and ductility. A finer grain matrix material forged at elevated temperatures maintains a lower flow stress, thus reducing cracking tendencies. The strength of the particle/matrix interface is not that critical since the fracture path typically occurs through the matrix. However, early fracture is possible when perturbation of flow around the large spherical particles is so significant that both high local shear strain and hydrostatic tension is generated between the particles. Fine SiC particles exhibit less damage than polycrystalline microspheres during forging. In addition, as shown in Fig. 2 (Ref 23), the forgeability of 2014 Al is lower than 6061 Al at 400 °C (750 °F) even though the 2014 has smaller-sized Al_2O_3 platelets. The lower forgeability of the 2014 suggests that matrix forgeability has a strong impact on the overall forgeability of the composite at elevated temperatures.

Much less work has been conducted on cold forming/forging, due to the more limited ductility of such materials, although hydrostatic extrusion of these materials is possible at room temperature (Ref 37, 38). In all cases, damage in the form of reinforcement cracking and/or reinforcement/matrix interface voiding may occur, even in compression. There is often a change in failure mechanism with increasing test temperature and/or strain rate. A number of studies have investigated the compressive behavior of DRA at room temperature and elevated temperature, both at quasi-static and dynamic strain rates. Room-temperature results are provided in Ref 5 and 7 to 13, while high-temperature results are found in Ref 7, 9, and 14 to 16.

Specific Results on Various DRA Systems

The following provides a summary of some of the specific results obtained on various DRA systems. Some of the most extensive work has been conducted on Al-Cu-Mg systems (i.e., 2*xxx*

Table 2 Recommended forging temperature ranges for aluminum alloys

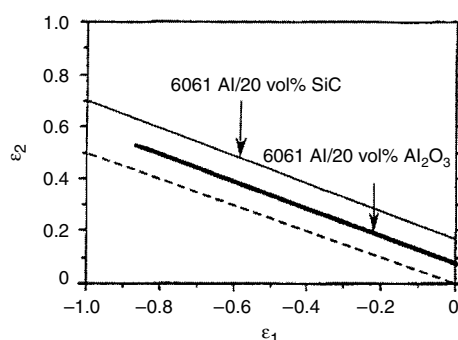| Aluminum alloy	Forging temperature range	
	°C	°F
1100	315–405	600–760
2014	420–460	785–860
2025	420–450	785–840
2219	425–470	800–880
2618	410–455	770–850
3003	315–405	600–760
4032	415–460	780–860
5083	405–460	760–860
6061	430–480	810–900
7010	370–440	700–820
7039	380–440	720–820
7049	360–440	680–820
7050	360–440	680–820
7075	380–440	720–820
7079	405–455	760–850

Source: Ref 4

Fig. 1 Forging-limit diagrams for 6061 Al/20 vol% SiC and 6061 Al/20 vol% Al_2O_3 tested at a strain rate of 0.5/s and 400 °C (750 °F). Source: Ref 23
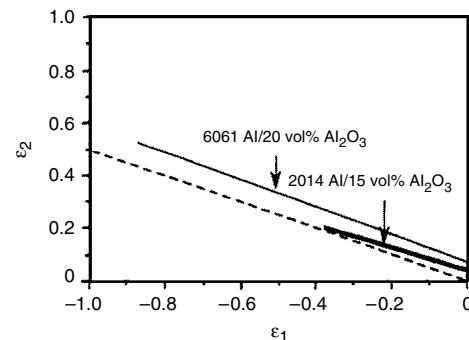

Fig. 2 Forging limit-diagrams of 6061 DRA and 2014 DRA tested at a strain rate of 0.5/s and 400 °C (750 °F). Source: Ref 23

series), although a summary of each of the systems investigated is reviewed below.

2xxx DRA Alloys. Forging of aluminum-copper-base metal-matrix composites reinforced with ceramic particles such as Al_2O_3 and SiC have been examined by several investigators (Ref 8, 9, 14, 15, 17). The form of these studies included developing the compressive stress versus strain response of the material under open-die forging conditions. Typical findings for these types of forging studies revealed an increased 0.2% offset yield strength with increasing strain rate, extensive particle cracking at elevated temperatures and strain rates, and densification in the case of powder forging of composites containing different levels of starting porosity.

Another study revealed that a fully dense P/M 2080 reinforced with 15% SiC (15 μm, or 0.6 mil) exhibited no macrocracking in subscale forged billets. However, forging of porous P/M 2080 reinforced with 20% SiC (9 μm, or 0.35 mil) showed different amounts of surface cracking in subscale billets forged to different strain levels at 500 °C (930 °F), as shown in Fig. 3 (Ref 5, 19–21). The outer portions of the forged billet may experience significant tensile stresses depending on the level of barreling, thereby producing cracking. No cracking was observed at low strain rates (Fig. 3), indicating that powder forging of some composites may be a viable near-net-shape manufacturing route. Furthermore, enhanced densification and no cracking was observed in the central region of billets shown in Fig. 3, regardless of strain rate. This apparently arises due to the presence of significant hydrostatic compressive stresses and again indicates that careful control of stress state should facilitate forging of both fully dense and porous composites. Densification in the central regions of the subscale forged billets was present even at the highest strain rates, shown in Fig. 4 (Ref 5, 19–21). Figure 3 illustrates the dependence of cracking on the external surfaces with increasing strain, where no cracking is observed at a true strain of 0.4 and extensive cracking is present at 0.7 strain. As expected, the densification behavior and powder forging characteristics of porous DRA composites is more complicated than forging of fully dense DRA composites since the former are affected by initial and evolving level of porosity; loading rate; reinforcement level, size, and homogeneity; test temperature; level of strain; and stress state present in various regions of the billet.

In the case of forging of a fully dense DRA, extensive particle cracking was also observed in both 2124 with 20 vol% SiC_p (14.5 μm, or 0.57 mil) and 2618 reinforced with 20 vol% Al_2O_3 (10 μm, or 0.4 mil) (Ref 9, 14). Figure 5 shows the manifestation of instability in the form of flow localization followed by extensive cracking indicated by the arrows (Ref 14). Clustering of the reinforcement in the 2618 Al/20 vol% Al_2O_3 inhibited the plastic flow of the material due to a reduction of maximum

stresses at the center of the clustered particles and the high levels of hydrostatic stress present in the clustered regions (Ref 9). Void formation preceded the clustering. Fracture of the particles

occurred when the maximum stress was reached. Increasing the forging temperature to 500 °C (930 °F) eliminated the cracking in the composite since the matrix ductility was restored
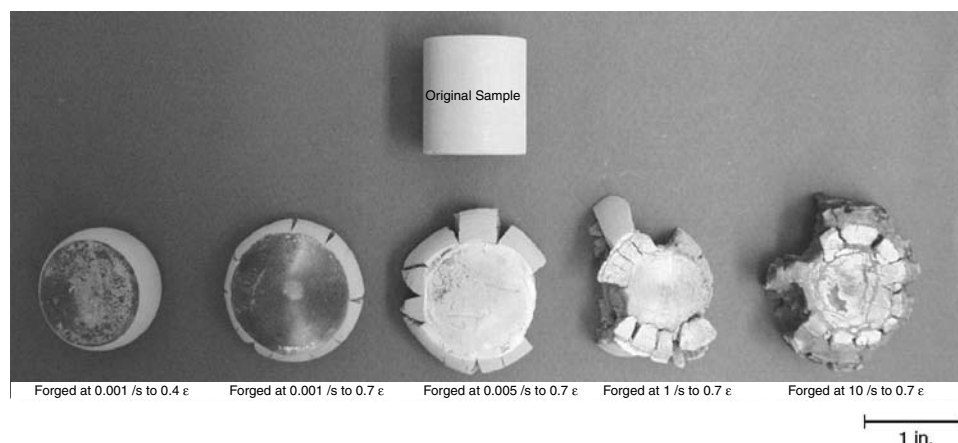

Forged at 0.001 /s to 0.4 ε   Forged at 0.001 /s to 0.7 ε   Forged at 0.005 /s to 0.7 ε   Forged at 1 /s to 0.7 ε   Forged at 10 /s to 0.7 ε

1 in.

Fig. 3 Macroscopic appearance of P/M 2080/20 vol% SiC powder compacts forged at different strain-rate/strain combinations at 500 °C (930 °F). Source: Ref 5
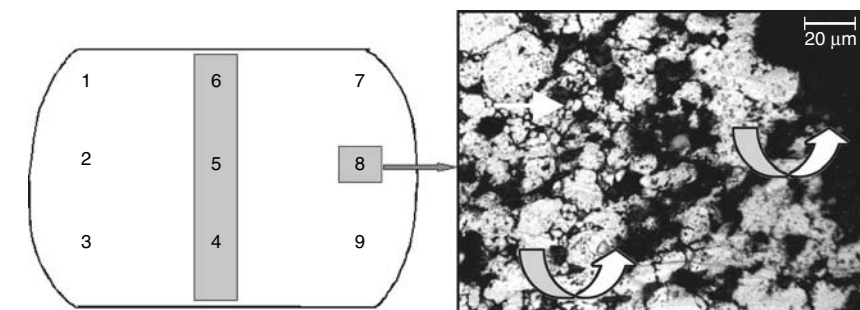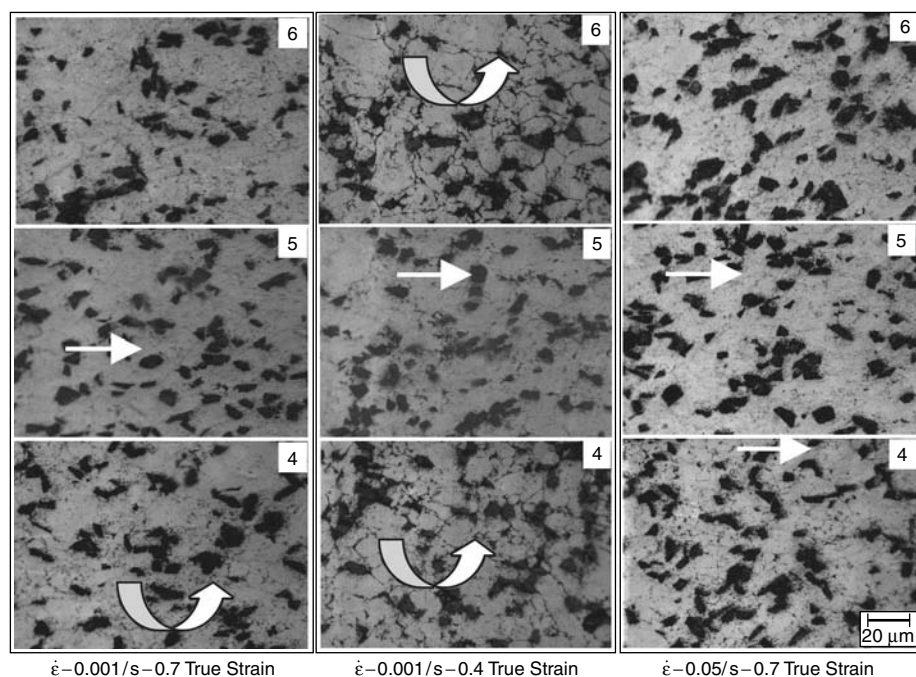

$\dot{\varepsilon}-0.001/s-0.7$ True Strain $\dot{\varepsilon}-0.001/s-0.4$ True Strain $\dot{\varepsilon}-0.05/s-0.7$ True Strain

Fig. 4 Microstructures in regions 4, 5, 6, 8 of the porous billets forged at different strain-rate/strain conditions at 500 °C (930 °F) for P/M 2080/20 vol% SiC. Straight arrows locate SiC, curved arrows show regions of porosity. Source: Ref 5

through various mechanisms such as dynamic recovery and recrystallization.

In another study (Ref 17), the presence of secondary tensile stresses in 2014 containing 15 vol% Al_2O_3 particles caused incipient cracks parallel to the compression direction (Fig. 6). The presence of incipient cracking at the surface of the deformed samples defined the forging limit of the composite in that study (Ref 17). Forging-limit diagrams were constructed for the 2014 composite as a function of temperature and strain rate. Figure 7 shows the experimentally determined forging limit diagrams of the 2014 composite tested at 300 and 400 °C (570 and 750 °F) (Ref 17).

Excellent forgeability at 340 to 440 °C (645 to 825 °F)/0.14 s^{-1} was found in 2124 reinforced with 26 vol% SiC particles (3 μm, or 0.12 mil) (Ref 15). Forged samples exhibited no cracking in the reinforcement or at the reinforcement/matrix interface (Ref 15). In addition, forging of the composite did not produce any increase in the percent of voids or fractured SiC particles. This probably arose due to the very small size of the SiC particles, as it is known that there is a size

Fig. 5 Microstructure of 2124 Al/20 vol% SiC_p deformed at 350 °C (660 °F) and 1 s^{-1} showing manifestation of instability as flow localization and cracking (marked by arrows). Source: Ref 14

dependence to the fracture of SiC particles in such systems (Ref 1–3, 39–42).

Other DRA Alloys. Although there is less information on the forging behavior of other DRA systems, a variety of studies have investigated the compressive behavior at different strain rates and/or test temperatures. Pure aluminum with 40 to 55 vol% Al_2O_3 (i.e., 5, 10, 29, 58 μm, or 0.2, 0.4, 1.1, 2.3 mil, particle size) produced by gas-pressure infiltration and tested in compression at a variety of different strain rates at room temperature revealed an increase in the flow stress of the dynamically compressed samples, due to the strain-rate sensitivity of the matrix (Ref 12). Precision density measurements were used to quantify damage accumulation. Damage accumulated primarily as a function of increasing strain due to particle cracking, followed by separation of broken-particle segments, with some evidence of limited matrix cavitation. Composites containing smaller particles exhibited higher flow stress and lower strain-rate sensitivity and accumulated less damage. Increasing the reinforcement level produced higher flow stress, strain-rate sensitivity, and increased rates of damage accumulation.

Al-Mg-Si alloy composites (e.g., 6061) containing 20 vol% Al_2O_3 and produced by molten metal mixing and direct chill casting have been examined at strain rates ranging from 0.1 to 10/s at 300 to 550 °C (570 to 1020 °F) (Ref 7). At 300 °C (570 °F), fracture was observed to be dominated by particle cracking, while interfacial debonding was prevalent at 550 °C (1020 °F). A maximum in the ductility was obtained at an intermediate temperature where particle cracking and interfacial debonding were both minimized. In all cases, the ductility was affected by hydrostatic stress, consistent with much previous work (Ref 37, 38, 43–52). Significant differences were observed between the ductility of cast and extruded DRA in these studies. This was attributed to the differences in spatial distribution of the reinforcing phase between the different processing conditions. Similar studies have revealed significant effects of processing conditions (Ref 6, 53) on subsequent reinforcement homogeneity and resulting properties. SiC whisker

reinforced 6061 tested in compression near the solidus of the matrix similarly revealed an increase in compressive stress with increasing strain rate, although the behavior was different in subsolidus versus supersolidus tests (Ref 16).

Al-Zn-Mg-Cu alloy P/M composites (e.g., 7093) containing 15 vol% SiC particulates have been tested under open-die conditions at room temperature as well as 500 °C (930 °F). At room temperature, true compressive strains in excess of 0.6 were achieved prior to macroscopic shear cracking in the subscale billet (Ref 5). At 500 °C (930 °F), no cracking was observed in subscale billets compressed to true strains of 0.7 at strain rates of 0.5/s and 10/s, using a novel forging simulator device (Ref 5). Significant effects of changes in strain rate on the 0.2% offset yield strength were obtained, and no visible cracks were present in the subscale billets. However, significant changes to the reinforcement distribution were noted in different regions of the subscale billet forged at 500 °C (930 °F) (Ref 5). Similar observations of reinforcement redistribution have been noted in 2618 composites during axisymmetric compression at different temperatures (Ref 8).

Cast DRA Alloys. In addition to the wrought aluminum compositions described previously, a variety of cast composites have been evaluated under similar conditions. Work on Al-Si-Mg die cast composites (Ref 18) revealed microstructure and mechanical property changes that accompanied various closed-die hot forging steps on as-cast material. The forged microstructures exhibited a more uniform distribution of SiC particles and the eutectic silicon in comparison to as-cast material. The forged materials similarly exhibited higher mechanical properties, consistent with earlier reports of beneficial effects of deformation processing on both microstructure and properties of A-356 20 vol% SiC composites (Ref 6).

Other work (Ref 16) on higher-rate compression testing of cast A-359 composites containing 20 vol% SiC with particle sizes ranging from 6 to 18 μm (0.24 to 0.8 mil) revealed a significant rate effect on strength. The composite exhibited a similar rate dependence as the monolithic matrix, but less strain hardening than the matrix,
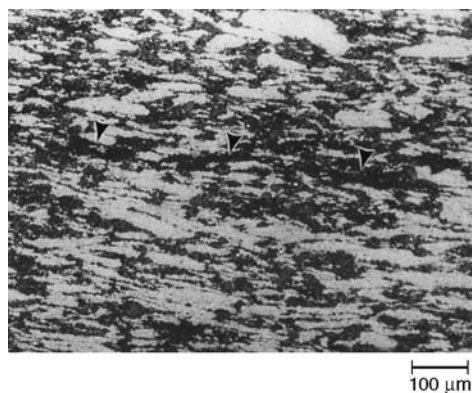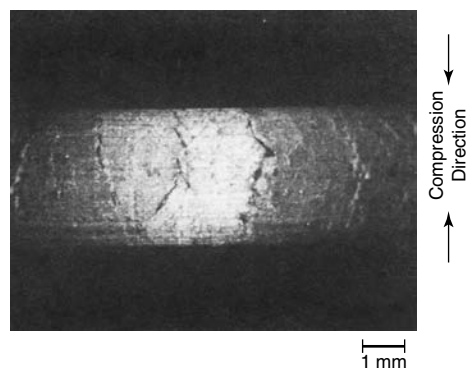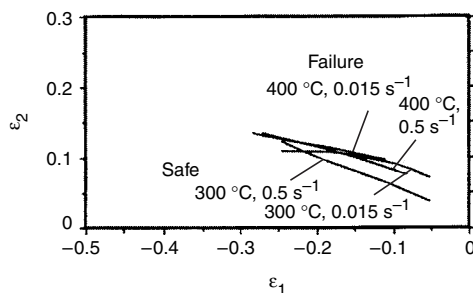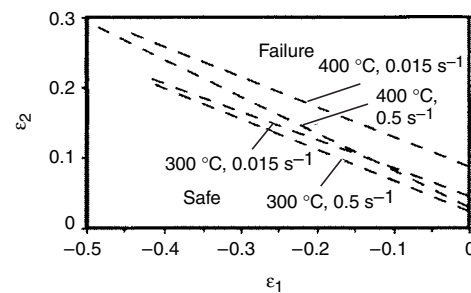

Fig. 6 Double-oblique cracking on a deformed 2014 Al/15 vol% Al_2O_3 forged at 250 °C (480 °F), strain rate of 0.1 s^{-1}, and true strain of $\ln(h_0/h) = 1.1$. Source: Ref 17

Fig. 7 Forging limit diagrams of 2014 Al/15 vol% Al_2O_3 at 300 and 400 °C (570 and 750 °F). (a) Samples had machined grids on the surface. (b) Samples had smooth surfaces. Source: Ref 17

apparently due to progressive particle fracture during compressive deformation at room temperature. The effects of submicrometer dispersions of 34 to 37 vol% Al_2O_3 on the compressive mechanical response of $Al-Al_2O_3$ composites indicated significant effects of reinforcement architecture and test temperature on behavior (Ref 10). At room temperature, an interconnected reinforcement architecture produced only modest increases in stiffness and strength compared to a discontinuous architecture of equal volume fraction. At higher test temperatures (e.g., 250, 500, and 600 °C, or 480, 930, and 1110 °F), the interconnected reinforcement was more effective at strengthening the composite. However, it was noted that the additional strengthening due to interconnectivity could only be exploited at small strains (e.g., <5%) due to the development of compressive flow instabilities in the composites with an interconnected reinforcement architecture. It was noted that microstructural damage controlled the instability strain of interconnected composites tested at room temperature, while the low strain-hardening coefficient controlled the appearance of flow instabilities in tests conducted at high temperatures.
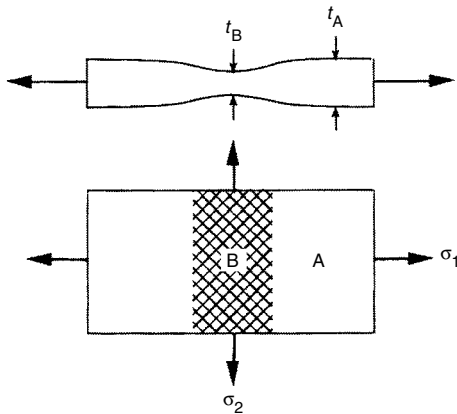

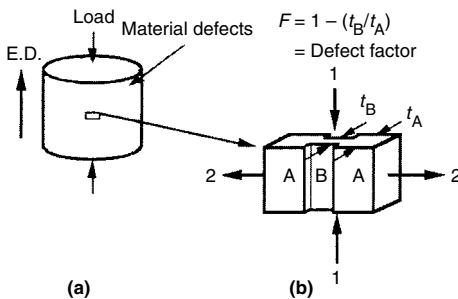**Fig. 8** Marciniak and Kucynski (MK) analysis. Source: Ref 55

Fig. 9 Modified Marciniak and Kucynski (MK) analysis for thin element containing surface defects of an upset sample. 1, compressive direction; 2, circumferential direction. Source: Ref 54
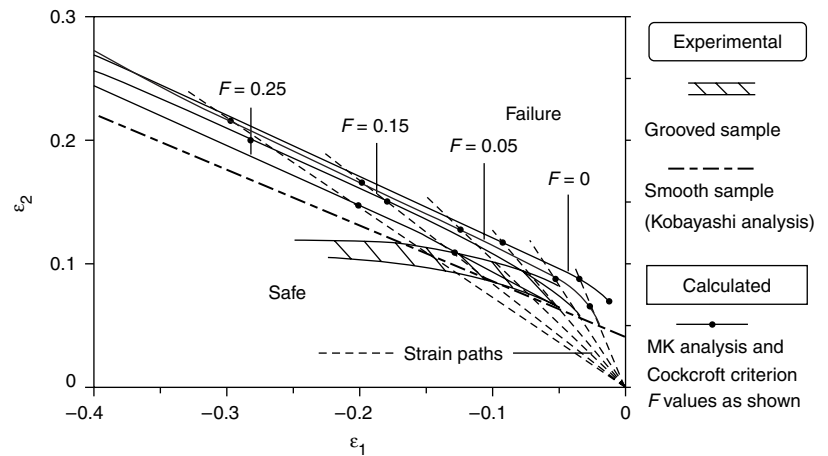

Fig. 10 Comparison of calculated and experimental forging limit diagrams for 2014 Al/15 vol% Al_2O_3 tested at a strain rate of 0.015/s and 300 °C (570 °F). Source: Ref 54

Fig. 11 Comparison of calculated and experimental forging limit diagrams for 2014 Al/15 vol% Al_2O_3 tested at a strain rate of 0.5/s and 400 °C (750 °F). Source: Ref 54
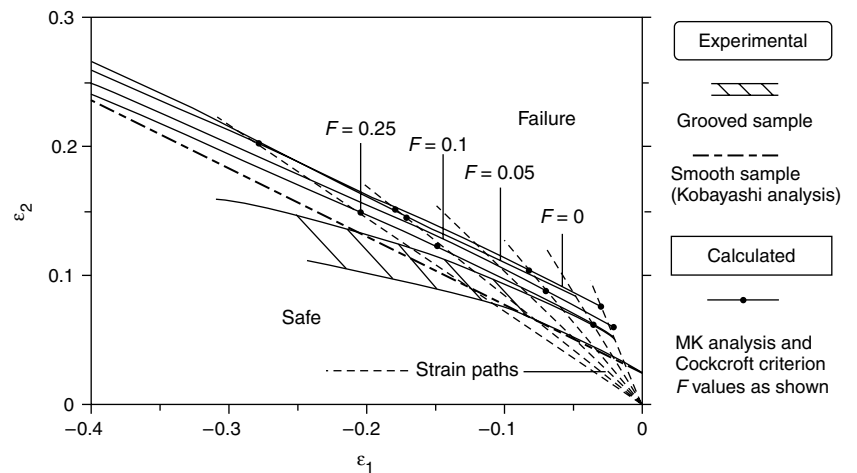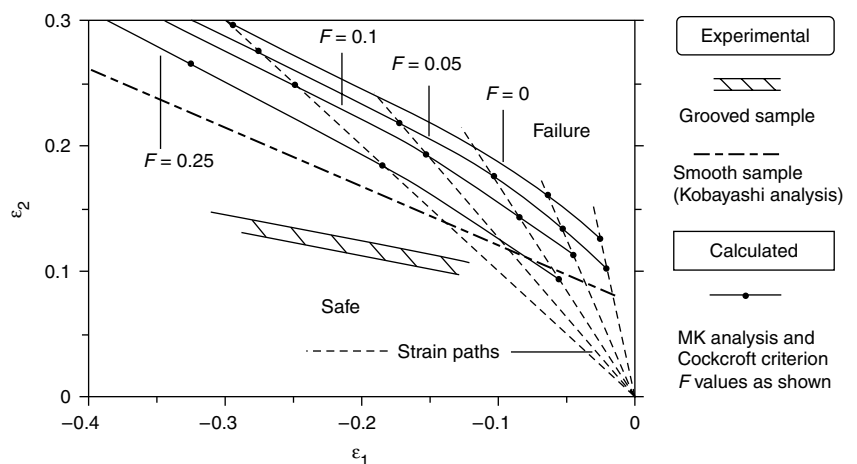

Fig. 12 Comparison of calculated and experimental forging limit diagrams for 2014 Al/15 vol% Al_2O_3 tested at a strain rate of 0.015/s and 400 °C (750 °F). Source: Ref 54

Modeling of Forging Behavior

As reviewed previously, a significant concern in forging composites is the presence of extensive cracking that can occur on the surface of the forged composite due to secondary tensile stresses. The presence of surface cracks is dependent on the amount of deformation induced in the forged composite. Syu and Ghosh (Ref 54) studied the forging limits in a 2014 Al with 15 vol% Al_2O_3 DRA. The study also included an attempt to compare the experimental work to calculated forging limits using plasticity analysis. Calculations were based on the flow-localization analysis of Marciniak and Kucynski (MK) (Ref 55) and various fracture criteria. Figure 8 shows a schematic diagram of the MK analysis assuming a groove exists perpendicular to the largest principal stress.

Syu and Ghosh (Ref 54) modified the MK analysis for a thin element containing defects near the surface of an upset sample shown in Fig. 9. Defects include nonuniform distribution of Al_2O_3 particles and matrix grain sizes, cracked Al_2O_3 particles, and porosity. The groove geometry is quantified by the defect factor, F, defined in Fig. 9. The defect factor evolves during the process of strain concentration between nondeformable particles and agglomerates.

Failure was assumed to be limited by fracture in the region of localized strain. Three fracture criterion were presented in this paper: Cockcroft-and-Latham fracture criterion (Ref 56), fracture-stress-based criterion (Ref 57), and constant effective fracture-strain criterion (Ref 54).

The Cockcroft-and-Latham fracture criterion proposes that ductile fracture occurs when the amount of deformation work due to the maximum tensile stress reaches a critical value C^*. The criterion is given in Eq 1, where σ_{2B} is the maximum tensile stress in region B, σ_{eff} and ε_{eff} are the effective stress and strain respectively, σ is the equivalent stress, ε is strain, and ε_f is the fracture strain in uniaxial tension. C^* is defined as the total deformation work possible without fracture.

$$\int_0^{\varepsilon_{eff}} \left(\frac{\sigma_{2B}}{\sigma_{eff}}\right)\sigma_{eff}\, d\varepsilon_{eff} > C^*, \text{ where } C^* = \int_0^{\varepsilon_f} \sigma d\varepsilon$$

(Eq 1)

The Cockcroft-and-Latham fracture criterion was found to be the most suitable criterion for this composite (Ref 54). A reasonably good match to the experimental forging limits at 300 °C (570 °F) with strain rates of 0.015 s^{-1} and 400 °C (750 °F) at a rate of 0.5 s^{-1} were found as shown in Fig. 10 and 11 (Ref 54).

Higher predictions for ε_2 and ε_1 were obtained at 400 °C (750 °F) with a strain rate of 0.015 s^{-1}, using the Cockcroft fracture criterion (Fig. 12). Reasons cited for the higher predicted values focused on possible changes in the fracture mechanism with increasing forging temperature. The Cockcroft criterion would not apply under these conditions since it does not consider diffusion creep, grain-boundary sliding, void initiation, or the interaction between particles and the matrix. All of these mechanisms could contribute to fracture in a composite and are not strictly considered in such a model.

Neither the fracture-stress-based criterion nor the effective-fracture-strain criterion was successful in predicting failure in these instances (Ref 57).

Properties of Deformation-Processed DRA Alloys

While a number of studies reviewed previously (Ref 5–10, 12, 14–21, 37–59) have investigated the effects of different processing parameters (e.g., strain rate, test temperature, stress state, etc.) on the flow stress response and damage development in subscale forgings of DRA, fewer studies have evaluated the resulting mechanical behavior of the subscale forged billets. In part, this relates to the difficulty of testing adequately sized subscale billets due to equipment capacity limitations. However, the general effects of deformation processing on subsequent microstructure and properties have been determined for both P/M and cast composites on a limited number of systems (Ref 5, 6, 18, 53). In addition, the availability of high-capacity forging simulation equipment (Ref 5) provides additional opportunities for studies of this type. It is clear from the preliminary studies (Ref 5) that reinforcement distribution is affected differently in different regions of the subscale billets forged under different conditions. This will likely affect a number of the mechanical properties, as has been demonstrated in some of the initial studies (Ref 5).

Recent investigations have explored the performance of sinter-forged P/M composites (Ref 35, 60–65). The microstructure of the sinter-forged composites exhibited relatively uniform distribution of SiC particles, which appeared to be somewhat aligned perpendicular to the forging direction. The sinter-forged composite exhibited higher Young's modulus and ultimate tensile strength than the extruded material, but lower strain to failure. The higher modulus and strength were attributed to the absence of any significant processing-induced particle fracture, while the lower strain to failure was caused by poorer matrix interparticle bonding compared to the extruded material. Fatigue behavior of sinter-forged composites was similar to that of the extruded material. A separate study (Ref 62) indicated that sinter forging at 530 °C (985 °F) for 100 min significantly increased the tensile strength and ductility of the composites. Hot rolling subsequent to the hot pressing produced no further increases to the ductility in that study (Ref 62).

REFERENCES

1. J.J. Lewandowski and P.M. Singh, Fracture and Fatigue of DRA Composites, *Fatigue and Fracture,* Vol 19, *ASM Handbook,* ASM International, 1996, p 895–904
2. J.J. Lewandowski, Fracture and Fatigue of Particulate MMC's, *Metal Matrix Composites,* T.W. Clyne, Ed., Vol 3, *Comprehensive Composite Materials,* A. Kelly and C. Zweben, Ed., Elsevier, 2000, p 151–187
3. T.W. Clyne and P.J. Withers, *An Introduction to Metal Matrix Composites,* Cambridge University Press, 1993
4. G.W. Kuhlman, Forging of Aluminum Alloys, *Forming and Forging,* Vol 14, *ASM Handbook,* ASM International, 1988, p 241–254
5. A. Awadallah, N.S. Prabhu, J.J. Lewandowski, Forging/Forming Simulation Studies on a Unique, High Capacity Deformation Simulator Apparatus, *Mater. Manuf. Process.,* Vol 17 (No. 6), 2002, p 737–764
6. G.A. Rozak, J.J. Lewandowski, J.F. Wallace, and A. Altmisoglu, Effects of Casting Conditions and Deformation Processing on A356 Aluminum and A356-20 vol.% SiC Composites, *J. Compos. Mater.,* Vol 26 (No. 14), 1992, p 2076–2106
7. P. Ganguly, W.J. Poole, and D.J. Lloyd, Deformation and Fracture Characteristics of AA6061 Particle Reinforced Metal Matrix Composites at Elevated Temperatures, *Scr. Mater.,* Vol 44, 2001, p 1099–1105
8. H. Xu and E.J. Palmiere, Particulate Refinement and Redistribution During the Axisymmetric Compression of an Al/SiCp Metal Matrix Composite, *Compos. Part A: Appl. Sci. Manuf.,* Vol 30, 1999, p 203–211
9. P. Cavaliere, E. Cerri, and E. Evangelista, Isothermal Forging Modeling of 2618+20% Al_2O_3p Metal Matrix Composite, *J. Alloy. Compd.,* Vol 378, 2004, p 117–122
10. M. Kouzeli and D.C. Dunand, Effect of Reinforcement Connectivity on the Elasto-Plastic Behavior of Aluminum Composites Containing Sub-micron Alumina Particles, *Acta Mater.,* Vol 51, 2003, p 6105–6121
11. Y. Li, K.T. Ramesh, and E.S.C. Chin, The Compressive Viscoplastic Response of an A359/SiCp Metal-Matrix Composite and of the A359 Aluminum Alloy Matrix, *Int. J. Solids Struct.,* Vol 37, 2000, p 7547–7592
12. C. San Marchi, F. Cao, M. Kouzeli, and A. Mortensen, Quasistatic and Dynamic Compression of Aluminum-Oxide Particle Reinforced Pure Aluminum, *Mater. Sci. Eng.,* Vol A337, 2002, p 202–211
13. S.M. Lee, J.H. Jung, E. Fleury, W.T. Kim, and D.H. Kim, Metal Matrix Composites Reinforced by Gas-Atomised Al-Cu-Fe Powders, *Mater. Sci. Eng.,* Vol 294–296, 2000, p 99–103
14. B.V. Radhakrishna Bhat, Y.R. Mahajan, H.Md. Roshan, and Y.V.R.K. Prasad, Processing Map for Hot Working of Powder 2124 Al-20 vol pct SiCp Metal Matrix

Composite, *Metall. Trans. A,* Vol 23A, 1992, p 2223–2230

15. C. Badini, G.M. La Vecchia, P. Fino, and T. Valente, Forging of 2124/SiCp Composite: Preliminary Studies of the Effects on Microstructure and Strength, *J. Mater. Process. Technol.,* Vol 116, 2001, p 289–297

16. G.S. Wang, L. Geng, Z.Z. Zheng, D.Z. Wang, and C.K. Yao, Investigation of Compression of SiCw/6061 Al Composites Around the Solidus of the Matrix Alloy, *Mater. Chem. Phys.,* Vol 70, 2001, p 164–167

17. D.G.C. Syu and A.K. Ghosh, Forging Limits for an Aluminum Matrix Composite: Part I. Experimental Results, *Metall. Mater. Trans. A,* Vol 25A, 1994, p 2027–2038

18. I. Ozdemir, U. Cocen, and K. Onel, The Effect of Forging on the Properties of Particulate-SiC-reinforced Aluminum-Alloy Composites, *Compos. Sci. Technol.,* Vol 60, 2000, p 411–419

19. E.J. Hilinski, J.J. Lewandowski, T.J. Rodjom, and P.T. Wang, Flow Behavior and Stress Evolution Modeling for Discontinuously Reinforced Composites, *1994 World P/M Congress,* Vol 7, C. Lall and A. Neupaver, Ed., Metal Powder Industries Federation, 1994, p 119–131

20. E.J. Hilinski, J.J. Lewandowski, T.J. Rodjom, and P.T. Wang, Development of a Densification Model for DRA Composites, *1994 World P/M Congress,* Vol 7, C. Lall and A. Neupaver, Ed., Metal Powder Industries Federation, 1994, p 83–93

21. E. Hilinski, J.J. Lewandowski, and P.T. Wang, Densification and Flow Stress Evolution Model for Powder Based DRA, *Aluminum and Magnesium for Automotive Applications,* J.D. Bryant, Ed., TMS-AIME, 1996, p 189–207

22. Y.V.R.K. Prasad and S. Sasidhara, *Hot Working Guide—A Compendium of Processing Maps,* ASM International, 1997

23. A.K. Ghosh, Solid-State Processing, *Fundamentals of Metal Matrix Composites,* S. Suresh, A. Moretensen, and A. Needleman, Ed., Butterworth-Heinemann, 1993, p 23–41

24. M.J. Koczak et al., Metal-Matrix Composites for Ground Vehicle, Aerospace, and Industrial Applications, *Fundamentals of Metal Matrix Composites,* S. Suresh et al., Ed., Butterworth-Heinemann, 1993, p 297–326

25. W.C. Harrigan, *Handbook of Metallic Composites,* S. Ochiai, Ed., Marcel Dekker, 1994, p 759–773

26. J. Eliasson and R. Sandstorm, Applications of Aluminum Matrix Composites, *Key Eng. Mater.,* Vol 104–107, 1995, p 3–36

27. C.J. Peel, Developments in Lightweight Aerospace Metallic Materials, Light Weight Alloys for Aerospace Applications III, E.W. Lee et al., Ed., TMS, 1995, p 191–205

28. M.V. Kevorkijan, MMCs for Automotive Applications, *Am. Ceram. Soc. Bull.,* Dec 1998, p 53–59

29. B. Maruyama, Progress and Promise in Aluminum Composites, *Adv. Mater. Process.,* Vol 156 (No. 1), 1999, p 47–50

30. F.H. Froes, *Light Metal Age,* Vol 5793–5794, 1999, p 48–61

31. W.H. Hunt, Jr., Metal Matrix Composites, *Design and Applications,* Vol 6, *Comprehensive Composite Materials,* A. Kelly and C. Zweben, Ed., Elsevier, 2000, p 57–66

32. W.H. Hunt, Jr., Metal Matrix Composites: Applications, *The Encyclopedia of Materials Science and Engineering,* Elsevier, 2001

33. W.H. Hunt, Jr. and D.B. Miracle, Automotive Applications of Metal-Matrix Composites, *Composites,* Vol 21, *ASM Handbook,* ASM International, 2001, p 1029–1031

34. S. Hurley, *Met. Bull. Mon.,* 1995, p 54–55

35. J.E. Allison and G.S. Cole, Metal-Matrix Composites in the Automotive Industry: Opportunities and Challenges, *JOM,* Vol 45, 1993, p 19–25

36. H.A. Kuhn and P.W. Lee, Fracture in Cold Upset Forging EM Dash a Criterion and Model, *Metall. Trans. A,* Vol 4, 1973, p 969

37. A.L. Grow and J.J. Lewandowski, Effects of Reinforcement Size on Hydrostatic Extrusion on MMC's, Paper No. 950260, *SAE Trans.,* 1995

38. J.J. Lewandowski and P. Lowhaphandu, Effects of Hydrostatic Pressure on Mechanical Behavior and Deformation Processing of Metals, *Int. Mater. Rev.,* Vol 43 (No. 4), 1998, p 145–188

39. P.M. Singh and J.J. Lewandowski, Effects of Heat Treatment and Particle Size on Damage Accumulation During Tension Testing of Al/SiC Metal Matrix Composites, *Metall. Trans. A,* Vol 24A, 1993, p 2451–2464

40. P.M. Singh and J.J. Lewandowski, Damage Evolution in DRA Materials, *Intrinsic and Extrinsic Fracture Mechanisms in Inorganic Composites,* J.J. Lewandowski and W.H. Hunt, Jr., Ed., TMS, 1995, p 57–69

41. J.J. Lewandowski and C. Liu, Microstructural Effects on Fracture Micromechanisms in Lightweight Metal Matrix Composites, *Proc. International Symposium on Adv. Structural Materials,* D. Wilkinson, Ed., Proc. Met. Soc. of Canadian Inst. Mining and Metallurgy, Vol 2, Pergamon Press, 1988, p 23–33

42. J.J. Lewandowski, C. Liu, and W.H. Hunt Jr., Effects of Microstructure and Particle Clustering on Fracture of an Aluminum Metal Matrix Composite, *Mater. Sci. Eng.,* Vol A107, 1989, p 241–255

43. J.J. Lewandowski, D.S. Liu, and M. Manoharan, Effects of Hydrostatic Pressure on Fracture of a Particulate Reinforced MMC, *Scr. Met.,* Vol 23, 1989, p 253–256

44. J.J. Lewandowski, D.S. Liu, and M. Manoharan, Effects of Microstructure on Fracture

of an Aluminum Alloy and an Aluminum Composite Tested under Low Levels of Superimposed Pressure, *Metall. Trans. A,* Vol 20A, 1989, p 2409–2417

45. J.J. Lewandowski and D.S. Liu, Pressure Effects on Fracture of Composites, *Lightweight Alloys for Aerospace Applications,* E.W. Lee, F.H. Chia, and N.J. Kim, Ed., TMS-AIME, 1989, p 359–364

46. M. Manoharan and J.J. Lewandowski, In-situ Deformation Studies of an Aluminum Metal Matrix Composite in a Scanning Electron Microscope, *Scr. Met.,* Vol 23, 1989, p 1801–1804

47. D.S. Liu, M. Manoharan, and J.J. Lewandowski, Matrix Effects on the Ductility of Aluminum Based Composites Tested under Hydrostatic Pressure, *J. Mater. Sci. Lett.,* Vol 8, 1989, p 1447–1449

48. D.S. Liu and J.J. Lewandowski, Effects of Superimposed Pressure on Mechanical Behavior of an MMC, *Proc. Second International Ceramic Science and Technology Congress—Advanced Composite Materials,* M.D. Sacks et al., Ed., 1990, p 513–518

49. J.J. Lewandowski, D.S. Liu, and C. Liu, Observations on the Effects of Particle Size and Superimposed Pressure on Deformation of Metal Matrix Composites, *Scr. Met.,* Viewpoint Set No. 15, Vol 25 (No. 1), 1991, p 21–26

50. D.S. Liu and J.J. Lewandowski, The Effects of Superimposed Hydrostatic Pressure on Deformation and Fracture: Part I 6061 Monolithic Material, *Metall. Trans. A,* Vol 24A, 1993, p 601–609

51. D.S. Liu and J.J. Lewandowski, The Effects of Superimposed Hydrostatic Pressure on Deformation and Fracture: Part II 6061 Monolithic Material, *Metall. Trans. A,* Vol 24A, 1993, p 609–617

52. A. Vaidya and J.J. Lewandowski, Effects of Confining Pressure on Ductility of Monolithic Metals and Composites, *Intrinsic and Extrinsic Fracture Mechanisms in Inorganic Composites,* J.J. Lewandowski and W.H. Hunt, Jr., Ed., TMS, 1995, p 147–157

53. T.M. Osman, J.J. Lewandowski, and W.H. Hunt, Microstructure-Property Relationships for an Al/SiC Composite with Different Deformation Histories, *Fabrication of Particles Reinforced Metal Composites,* J. Masonnave and F.G. Hamel, Ed., ASM International, 1990, p 209–216

54. D.G.C. Syu and A.K. Ghosh, Forging Limits for an Aluminum Matrix Composite: Part II. Analysis, *Metall. Mater. Trans. A,* Vol 25A, 1994, p 2039–2048

55. Z. Marciniak and K. Kuczynski, Limits Strains in the Processes of Stretch-Forming Sheet Metal, *Int. J. Mech. Sci.,* Vol 9, 1967, p 609–620

56. M.G. Cockcroft and D.J. Latham, Ductility and the Workability of Metals, *J. Inst. Met.,* Vol 96, 1968, p 33–39

57. V. Vujovic and A.H. Shabaik, New Workability Criterion for Ductile Metals, *ASME J. Eng. Mater. Technol.,* Vol 108, 1986, p 245–249

58. V.V. Bhanu Prasad, B.V.R. Bhat, Y.R. Mahajan, and P. Ramakrishnan, Hot Forging of Discontinuously Reinforced Aluminum Matrix Composites, *Mater. Sci. Technol.,* 2005, in press

59. V.V. Bhanu Prasad, B.V.R. Bhat, Y.R. Mahajan, and B.P. Khasyap, High Temperature Deformation Behavior and Processing Map of an Al/SiC Composite, *Metall. Trans. A,* 2005, in press

60. F.P. Liu, S. Papaefthimian, S. Luk, and W.H. Hunt, Jr., Forged P/M Connecting Rod Development Using Aluminum Metal Matrix Company, *Proceedings of the Second International Powder Metallurgy Aluminum & Light Alloys for Automotive Applications Conference,* Metal Powder Industries Federation, 2000, p 153–161

61. W.H. Hunt, Jr., New Directions in Aluminum-based P/M Materials for Automotive Applications, *Int. J. Powder Metall.,* Vol 36 (No. 6), 2000, p 51–60

62. N. Zhao and P. Nash, The Processing of 6061 Aluminum Alloy Reinforced SiC Composites by Cold Isostatic Pressing, Sintering and Sinter-Forging, *Proceedings of the Second International Powder Metallurgy Aluminum & Light Alloys for Automotive Applications Conference,* Metal Powder Industries Federation, 2000, p 145–152

63. Z. Ishijima, H. Shikata, H. Urata, and S. Kawase, Development of P/M Forged Al-Si Alloy for Connecting Rod, *Advances in Powder Metallurgy and Particulate Materials,* Vol 4, Metal Powder Industries Federation, 1996, p 14.3–14.13

64. M.S. Otsuki, S. Kakehashi, and T. Kohno, Powder Forging of Rapidly Solidified Aluminum Alloy Powders and Mechanical Properties of their Forged Parts, *Advances in Powder Metallurgy,* Vol 2, Metal Powder Industries Federation, 1990, p 345–349

65. N. Chawla, J.J. Williams, and R. Saha, Mechanical Behavior and Microstructure Characterization of Sinter-Forged SiC Particle Reinforced Aluminum Matrix Composites, *J. Light Met.,* Vol 2, 2002, p 215–227